J Mater Sci (2011) 46:7784–7792
DOI 10.1007/s10853-011-5758-3

Structural properties and kinetics of nitro-niobized steels

Saduman Sen · Kadir Kocaman

Received: 1 March 2011 / Accepted: 29 June 2011 / Published online: 13 July 2011

Abstract In the present study, structural characterization and kinetics of nitro-niobized AISI 1010, AISI D2, and AISI M2 steels by thermo-reactive deposition technique in the powder mixture consisting of ferro-niobium, ammonium chloride, and alumina at the temperatures of 1173, 1273, and 1373 K for 60–240 min were investigated. The thickness of the niobium nitride layers formed on the nitro-niobized AISI 1010, AISI D2, and AISI M2 steels are ranged from 2.80 ± 0.90 to 11.89 ± 1.10 μm, 3.16 ± 0.60 to 13.16 ± 1.51 μm, and 3.85 ± 0.91 to 16.77 ± 2.10 μm, respectively. The phases formed in the coating layer deposited on the surface of the steel substrates are $NbN_{0.95}$ and Nb_2CN. The hardness of the niobium nitride coating layers produced on AISI 1010, AISI D2, and AISI M2 steels are changing from 1151 ± 126 to 1446 ± 121 $HV_{0.005}$, 1359 ± 413 to 1594 ± 761 $HV_{0.005}$, and 1321 ± 51 to 1915 ± 134 $HV_{0.005}$, respectively. Diffusion constants of the coating layers were changing between 1.517×10^{-15} and 2.043×10^{-14} m^2/s, depending on steel compositions, treatment time and temperatures, and activation energies of the AISI 1010, AISI D2, and AISI M2 steels for the process were calculated as 128.7, 123.8, and 132.5 kJ/mol, respectively. Moreover, an attempt was made to investigate the possibility of predicting the contour diagram of niobium nitride coating thickness variation, depending on process time and temperature.

S. Sen (✉) · K. Kocaman
Department of Metallurgy and Materials Engineering,
Sakarya University, Engineering Faculty, Esentepe Campus,
54187 Sakarya, Turkey
e-mail: sdmnsen@sakarya.edu.tr

Introduction

Transition metal nitrides and carbides exhibit an attractive combination of physical, chemical, and mechanical properties which make them promising candidates for many technical applications. Especially as thin films, transition metal nitrides on metals are well-suited for improving the performance of cutting tools and drills due to their high hardness and wear resistance [1].

Among nitride coatings, niobium nitride (NbN) and NbN-based coatings are of increasing interest because of their high hardness, wear resistance, and superconducting properties [2–7]. Niobium nitrides are potential candidates for use in various cryogenic devices like high resolution X-ray detectors and electromagnetic radiation detectors ranging from millimeter wavelength to visible light. Their relatively high superconducting critical temperature allows them to be used as diffusion barrier in Josephson junctions and as coating for super conductive cables. Also, their high hardness, remarkable corrosion resistance, as well as good chemical stability at high temperature (1000 °C) explains that these compounds are often used as protective layers in active environment such as craft-space [7]. There are many coating techniques of Niobium nitride coatings, such as reactive magnetron sputtering [8–10], ion beam assisted processes [11], unbalanced magnetron [12], pulsed laser deposition [13], and vacuum arc deposition [14].

To control the thermo-chemical coating processes in automatic installations, knowledge of kinetic parameters is essential [15]. Some kinetic models have been developed for the establishment of the variables that affect the coating process. It is very important to establish the variables that affect the thermo-chemical coatings kinetics process to control automated procedures and obtain desirable properties [10].

The main objective of this study was to produce niobium nitride thin layer on AISI 1010, AISI D2, and AISI M2 steels by a two-step treatment. The first step is a gas nitriding treatment for producing iron nitride phases and solid solution of nitrogen on the substrate. The second step is a niobizing treatment for producing niobium nitride phases on the pre-nitrided steels.

Experimental procedures

AISI 1010, AISI D2, and AISI M2 steels were used as substrates for niobium nitride coating by thermo-reactive deposition technique. AISI 1010, AISI D2, and AISI M2 steels were selected for niobium nitride coating which can be used for the increase service performance of these steels. It is well known that AISI 1010 steel is a plain low-carbon steel which can be used for surface hardening steel either by carburizing or nitriding processes; AISI D2 steel is a famous cold work tool steel which is widely used for mold manufacturing, and AISI M2 steel is a famous high-speed steel which is used for cutting tools. The chemical compositions of these steels were given in Table 1. The substrate samples were in the form of cylindrical coupons that have a dimension of 20 mm in diameter and 5 mm in thickness, and polished progressively with 1200 grit emery papers. Then, these samples were cleaned ultrasonically in acetone and dried.

AISI 1010, AISI D2, and AISI M2 steels were gas nitrided for the purpose to rich the surfaces with nitrogen of the steels in a nitrogen and ammonia atmosphere at 803 K for 120 min in a tube furnace. Then, niobium nitride coating was performed on the pre-nitrided steel samples by thermo-reactive deposition (TRD) process. The TRD process was performed utilizing a pack box containing ferro-niobium, ammonium chloride, and alumina powders, in a high temperature tube furnace cleaned by vacuum and then argon gases. Ferro niobium, ammonium chloride, and alumina were used as a metal supplier (Nb), activator, and filler materials, respectively. Possible reactions took place in the coating bath for the niobium nitride coating is given as follows [16–21]:

$$NH_4Cl_{(s)} = NH_{3(g)} + HCl_{(g)} \quad (1)$$

$$2NH_{3(g)} = N_{2(g)} + 3H_{2(g)} \quad (2)$$

$$Nb_{(s)} + 5HCl_{(g)} = NbCl_{5(g)} + 5H^{+}_{(g)} \quad (3)$$

$$NbCl_{5(s)} + 5/2H_{2(g)} = Nb_{(g)+}5HCl_{(g)} \quad (4)$$

$$3NbCl_{5(g)} + 5Fe_{(s)} = 5FeCl_{3(g)} + 3Nb_{(g)} \quad (5)$$

$$Nb_{(g)} + Fe_xN_{(s)} = NbN_{(s)} + XFe \quad (6)$$

$$Nb_{(g)} + C_{(s)} = NbC_{(s)} \quad (7)$$

$$NbN_{(s)} + NbC_{(s)} = Nb_2CN_{(s)} \quad (8)$$

The major process parameters are presented in Table 2.

Niobium nitride coated samples were sectioned from one side and prepared metallographically up to 1200 grid emery paper, and then polished using 1 μm alumina paste. Polished samples were etched by 3% Nital before tests. The thickness of coating layers and their morphologies were examined using NIKON EPIPHOT optical microscopy and JEOL 6060 LV scanning electron microscopy (SEM) on the cross-sections of the niobium nitride coated samples. The phase analysis of the pre-nitrided layers and niobium nitride coating layers were determined by X-ray diffraction analysis using RIGAKU XRD D/MAX/2200/PC X-ray diffractometer employing Cu K_α radiation. The hardness of the coated steels was also measured using a FUTURE

Table 2 Process parameters of niobium nitride coating

Deposition parameters	Value
Nitriding temperature (K)	803
Nitriding time (min)	120
Nitriding gas mixture	Nitrogen and ammonia
Niobium nitride coating temperature (K)	1173, 1273, and 1373
Niobium nitride coating time (min)	60, 120, 180, and 240
Pack content (Ferro-Niobium/ammonium chloride/alumina (by wt%)	2/1/2
Cooling time (min)	60

Table 1 Chemical compositions of steel substrates

Steel	Chemical composition (%, by weight)									
	C	Si	Mn	P	S	Cr	Ni	Mo	W	V
AISI 1010	0.12	0.11	0.05	0.003	0.023	0.012	0.029	0.02	–	–
AISI D2	1.43	0.29	0.20	0.005	0.005	11.38	0.68	0.60	0.01	–
AISI M2	0.71	0.47	0.27	0.038	0.025	3.45	0.12	3.45	14.77	1.55

TECH FM 700 micro-hardness tester fitted with a Vickers indenter under the loads of 5 gf. Contour diagrams of the niobium nitride coating layers in relation to treatment time and temperature were examined using SigmaPlot 11 software.

Results and discussion

Coating characterization

Both optical and SEM cross-sectional examinations of the niobium nitride coated AISI 1010, AISI D2, and AISI M2 steels show that coating layers formed on the steel samples include compact layers on the top and sub-layer, while the mid-layer of the coatings are a spongy structure. Coating layers are also well bonded to the substrate and crack free, as shown in Fig. 1. There were three distinct regions visible at higher magnifications on the cross-section of the niobium nitride coated steels, They are (i) a surface coating layer consisting of $NbN_{0.95}$ and Nb_2CN phases which were confirmed by X-ray diffraction analysis, as seen in Fig. 2. The phases formed in the coating layers of the nitro-niobized AISI 1010, AISI D2, and AISI M2 are changing with the steel compositions. While the coating layer of the nitro-niobized AISI 1010 steel is including $NbN_{0.95}$ phase as a major phase, AISI D2 and AISI M2 steels have a Nb_2CN phase as a major phase as seen in the Fig. 2. Carbon content of the AISI D2 and AISI M2 steels are much higher than that of the AISI 1010 steel. It is possible that the carbon diffuse in the nitro-niobized layer from the pre-nitrided steels together with nitrogen atom and so, Nb_2CN phase can form dominantly in the coating layer instead of $NbN_{0.95}$ phase. In addition, it is possible that the phases took place in the nitro-niobized layers of the steels were undoubtedly influenced from the pre-nitrided layer

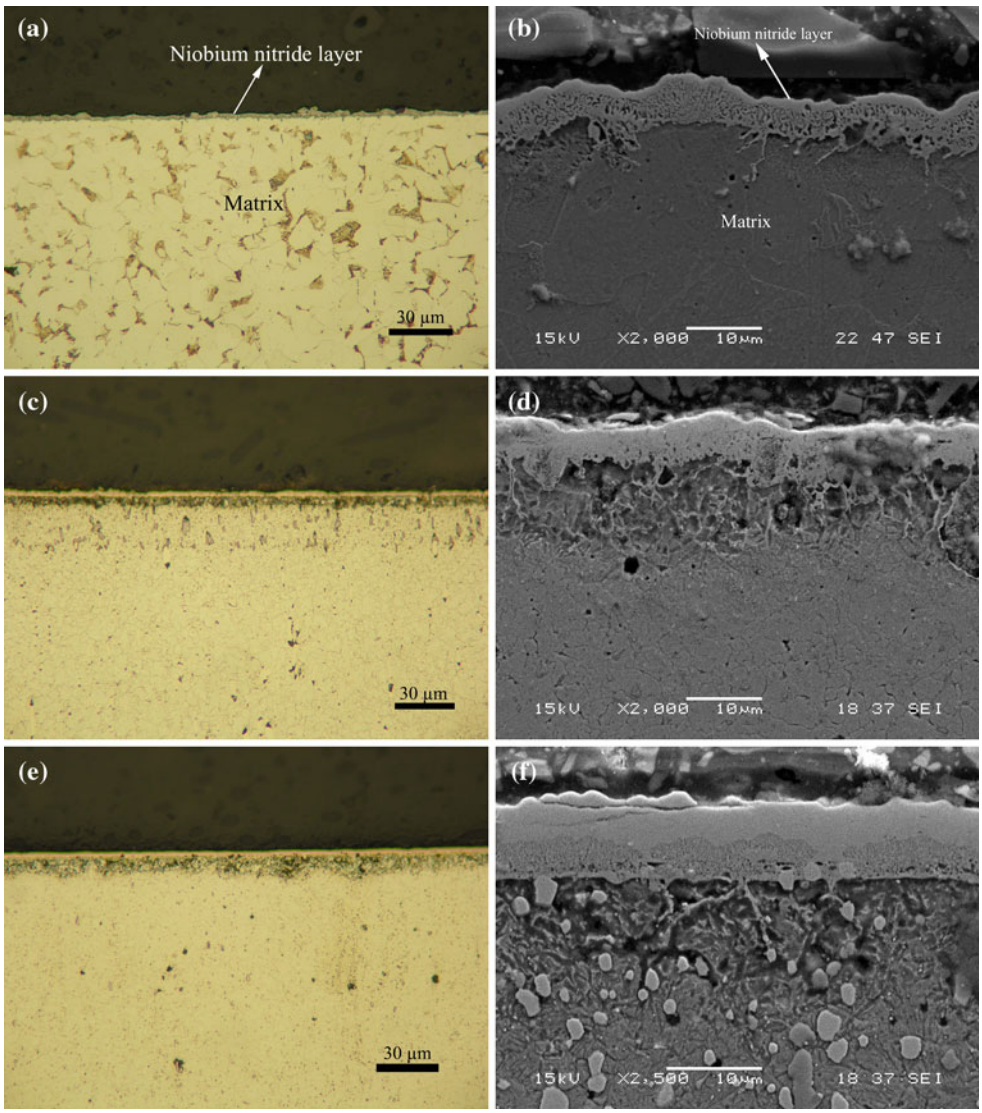

Fig. 1 Optical and SEM micrographs of the nitro-niobized AISI 1010 (**a, b**), AISI D2 (**c, d**), and AISI M2 (**e, f**) steels at 1273 K for 120 min, respectively

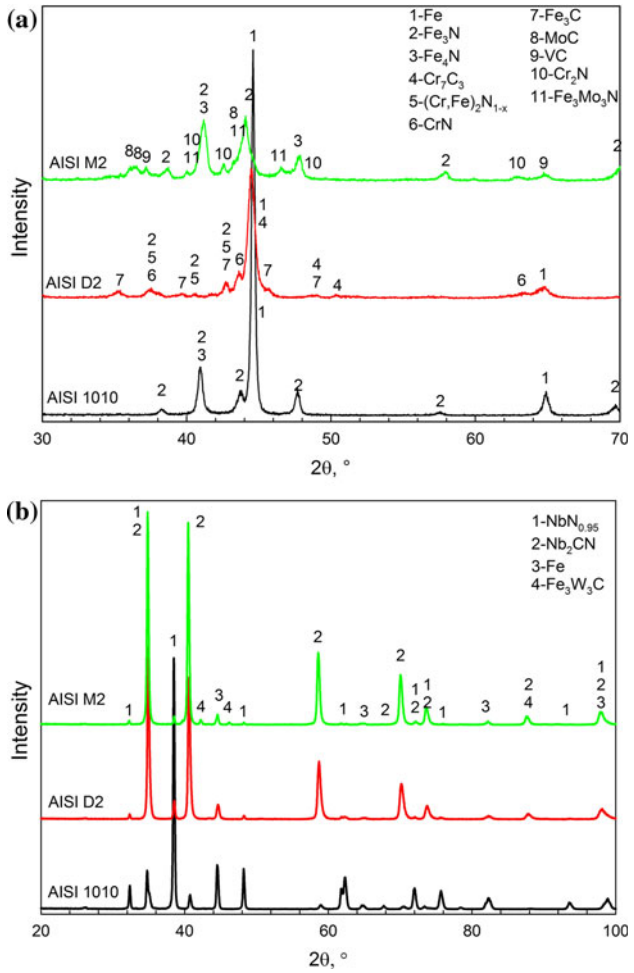

Fig. 2 X-ray diffraction patterns for **a** pre-nitrided and **b** nitro-niobized steels at 1273 K for 120 min

composition. As seen from the X-ray diffraction analysis of the pre-nitrided steels, there are a lot of nitride and carbide phases took place in the nitrided layers of the AISI D2 and AISI M2 like Fe_3N as a major phase, Fe_4N, Cr_7C_3, $(Fe,Cr)_2N_{(1-x)}$, CrN, Fe_3Mo_3N, MoC, VC, etc. (minor phases), see Fig. 2a; (ii) transition zone which includes some porosity that is able to caused from the nitrogen migration from the nitride zone of the substrate. As known, TRD process includes the migration of carbon and nitrogen elements from matrix to the surface, when carbide or nitride forming elements like chromium, titanium, niobium, vanadium, etc. migrates from coating bath to the substrate surface. Therefore, the chemical composition of the coating layer can be changed with alloying elements of the steels and some porosity can be realized near the coating layer in the matrix [22, 23]; (iii) steel matrix which is not affected by niobium. The hardness values of uncoated steels and niobium nitride layer formed on nitro-niobized AISI 1010, AISI D2, and AISI M2 steels are given in Table 3. The hardness of the coating layers and matrix

Table 3 Hardness values for substrate and coating layers

Steel	Substrate hardness ($HV_{0.3}$)	Coating layer hardness ($HV_{0.005}$)	Change, % (max)
AISI 1010	130	1151 ± 126 to 1446 ± 121	1012 (↑)
AISI D2	670	1359 ± 413 to 1594 ± 761	138 (↑)
AISI M2	746	1321 ± 51 to 1915 ± 134	157 (↑)

of the nitro-niobized steels at 1273 K for 120 min is shown in Fig. 3. The hardness values of nitro-niobized layers are much higher than that of the substrates. In the present study, the hardness of niobium nitride layers ranged from 1151 to 1915 $HV_{0.005}$, depending on process parameters and steel compositions. The phases took place in the coating layer are changing with steel compositions as mentioned above. Therefore, the hardness of the nitro-niobized layers increase with the increase in alloying elements of the nitro-niobized steels. AISI 1010 plain carbon steel does not have any carbide-forming elements, and the dominant phase formed in the coating layer of the nitro-niobized layer is $NbN_{0.95}$. Whereas, nitro-niobized layer of the AISI D2 and AISI M2 steels include the Nb_2CN phase as a dominant phase beside $NbN_{0.95}$. In addition, it is possible that the alloying elements of the steels may have played a role on the coating layer hardness dissolved in the coating layer, too. Klingenberg et al.'s study [11] showed that the hardness values of niobium nitride coating realized by IBAD technique were changing between 370 and 2390 HV depending on the process parameters. The hardness results are in good agreement with the present study. Pei et al. [24] explained that the hardness values of the NbC, Nb_2C, NbN, Nb_2N phases are found to be 1961, 2123, 1396, and 1720 HV, and these phases have a similar crystal structure [25]. Wong et al.'s study [26] showed that

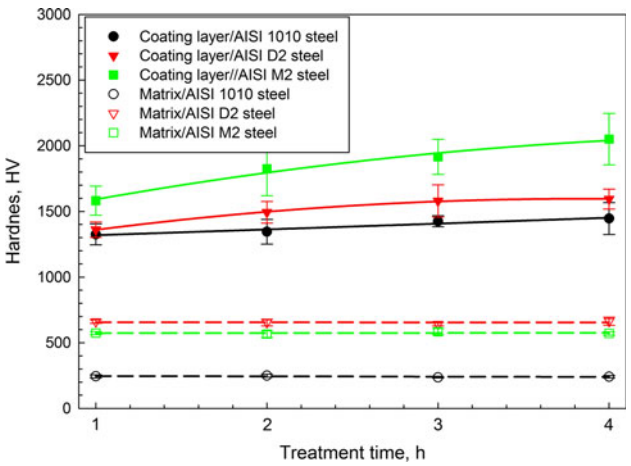

Fig. 3 Hardness values for the steel substrates and coating layers at 1273 K for 120 min

the hardness of niobium nitride layer were changing between 1700 and 4100 HV, depending on nitrogen partial pressure and process parameters. As shown in Table 3, the hardness of the coating layers formed on AISI 1010, AISI D2, and AISI M2 steels were increased about 1012, 138, and 157% according to the substrate hardness of the steels, respectively.

Kinetics studies

Depending on the niobizing temperature and time, the thickness of niobium nitride layers formed on the nitro-niobized AISI 1010, AISI D2, and AISI M2 steels are ranged from 2.80 ± 0.90 to 11.89 ± 1.10 μm, 3.16 ± 0.60 to 13.16 ± 1.51 μm, and 3.85 ± 0.91 to 16.77 ± 2.10 μm as shown in Figs. 4, 5, and 6, respectively. Increase in alloying elements in the steel substrates resulted

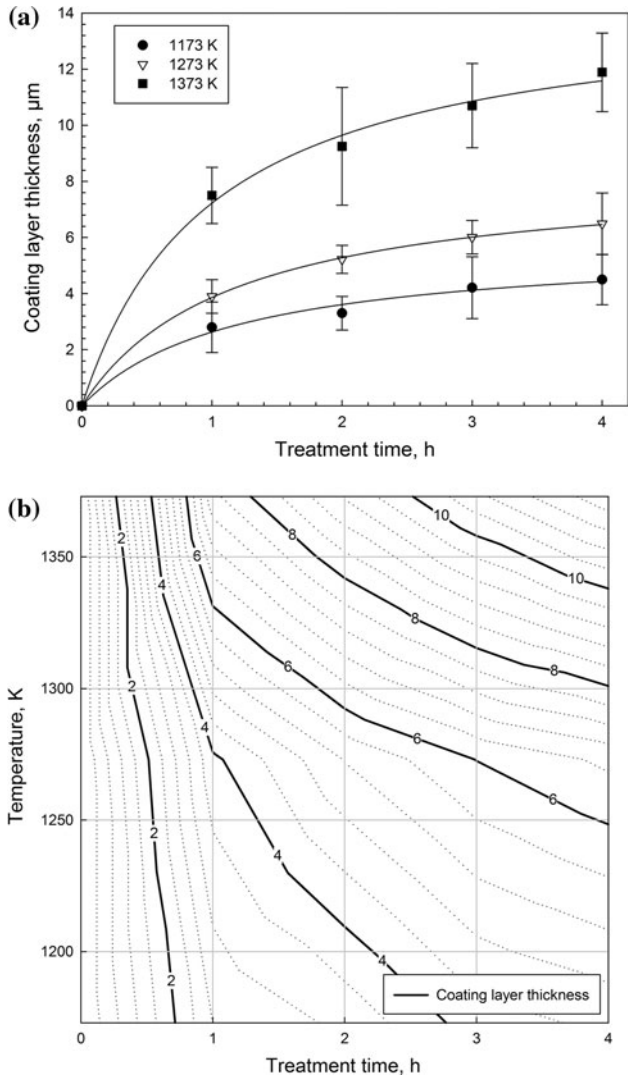

Fig. 4 The thickness (**a**) and contour diagrams (**b**) of niobium nitride layers of nitro-niobized AISI 1010 steel

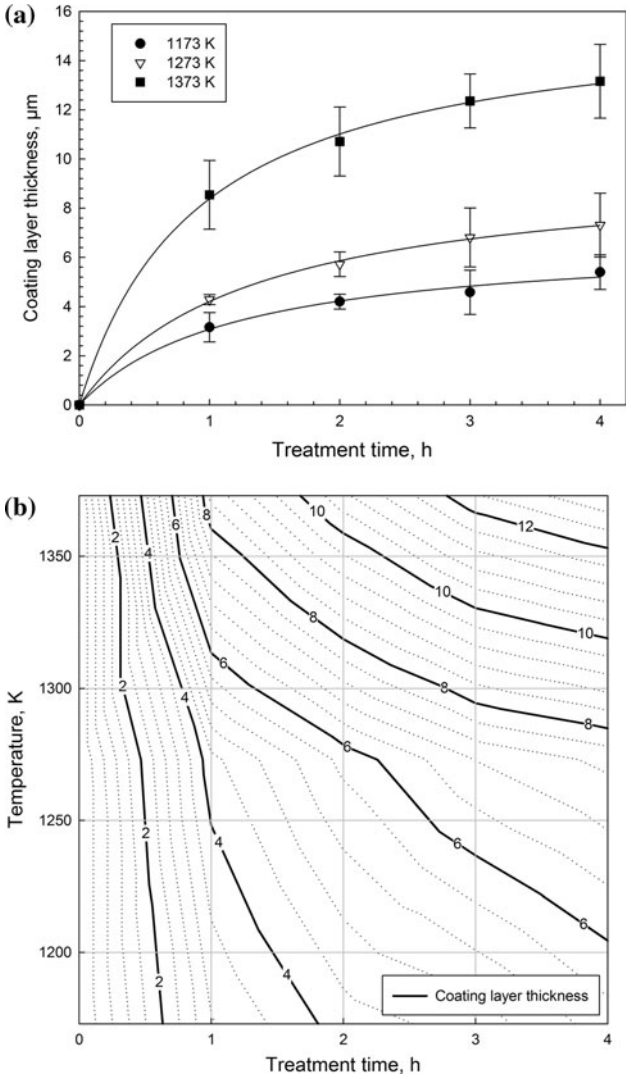

Fig. 5 The thickness (**a**) and contour diagrams (**b**) of niobium nitride layers of nitro-niobized AISI D2 steel

to thicker coating layer for the same process conditions. It is possible that the alloying elements took place in the steel samples could encourage the thicker niobium nitride layers formation. The microstructure and mechanical properties of the coating layers strongly depend on the chemical composition of the base metal in thermo-chemical coating process [27, 28]. In general, the thickness of the coating layer realized by thermo-chemical coating processes, such as boronizing or nitriding treatments, decreases with an increase in alloying elements [29]. On the contrary, in the present study, increase in alloying elements in the steel compositions increased the coating layer thickness. Pre-nitrided AISI D2 and AISI M2 steels include some alloying elements nitrides and carbides mentioned above. These phases have a similar crystal structure with the niobium nitride phases [25]. The nitride and carbide phases took place in the nitrided layers of the AISI D2 and AISI M2

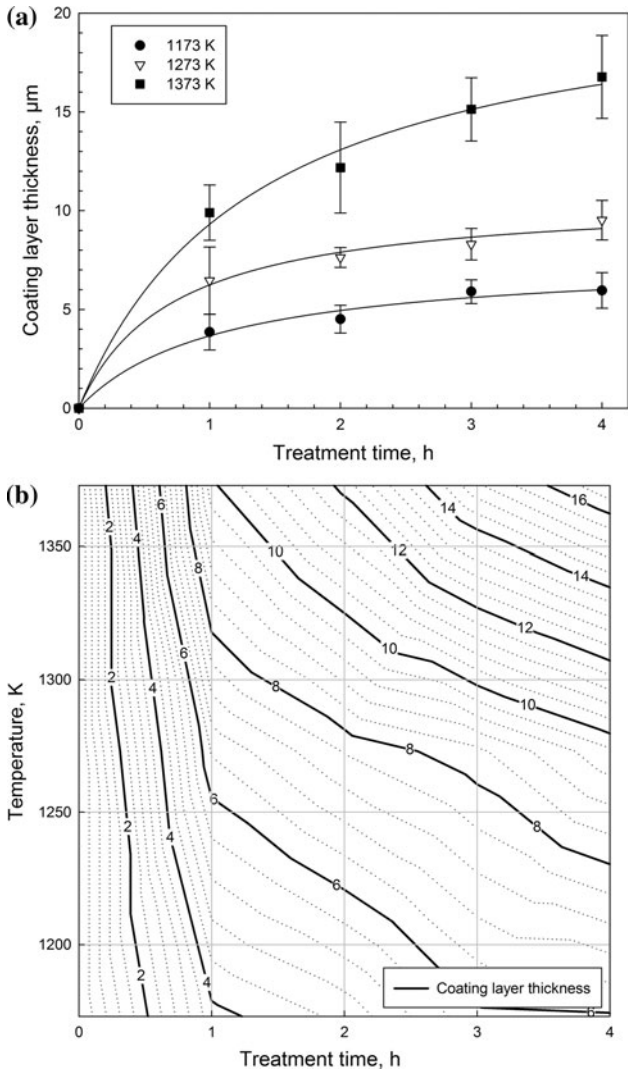

Fig. 6 The thickness (**a**) and contour diagrams (**b**) of niobium nitride layers of nitro-niobized AISI M2 steel

steels are possible to have a heterogeneous nucleation zone effect for the formation of niobium nitride coating and so, encouraged the coating layer thickness increment with increase in alloying elements. Similar behavior was shown on the nitro-titanizing treatment realized on AISI 1010 and AISI M2 steels realized by Deniz study [30]. Deniz study showed that the increase in alloying elements in the steel samples caused the increase in nitro-titanized layer thickness in the thermo-reactive deposition process. In the thermo-chemical coating process, transition zones took place under the coating layers include the diffused elements. As known, diffusion of interstitial elements like C, N, and B are much more than that of the substitutional atom in the steel matrix. Therefore, it is possible that the nitrogen and carbon atoms have an effective diffusion than that of the niobium in the nitro-niobizing treatment [31]. It is clearly shown that niobium nitride layer thickness increases parabolically with niobizing time at a given process temperature. In addition, contour diagrams were established using the data of Figs. 4, 5, and 6b can be used for two purposes: (i) to predict the coating layer thickness with respect to the process parameters, namely time and temperature; (ii)to determine the process time and temperature for obtaining a predetermined coating layer thickness [32].

From the niobium nitride layer thickness data of nitro-niobized steels, the growth rate constant of niobium nitride coatings was calculated for each temperature using Eq. 1 [33].

$$d^2 = K.t \qquad \text{(Eq.1)}$$

where, t is niobizing time (s) and K is the growth rate constant that depends on the diffusion element (in this case, niobium). If the kinetics of layer formation for a period between 60 and 240 min is considered, it can be recognized that the square of niobium nitride layer thickness changes linearly with time as shown in Figs. 7, 8, and 9.

The relationship between the diffusion coefficients (growth rate constant), K (m^2/s), activation energy, Q (J/mol), and the process temperature in Kelvin, T, can be expressed as an Arrhenius equation [34]:

$$K = K_O.e^{-\frac{Q}{RT}} \qquad \text{(Eq.2)}$$

where, K_o is the frequency factor (pre-exponential constant) and R is the gas constant J/(mol K). Taking the natural logarithm of Eqs. 2 and 3 can be derived as follows:

$$\ln K = \ln K_O - \frac{Q}{RT} \qquad \text{(Eq.3)}$$

Consequently, the activation energy for the niobium diffusion in the niobium nitride layer is determined by the

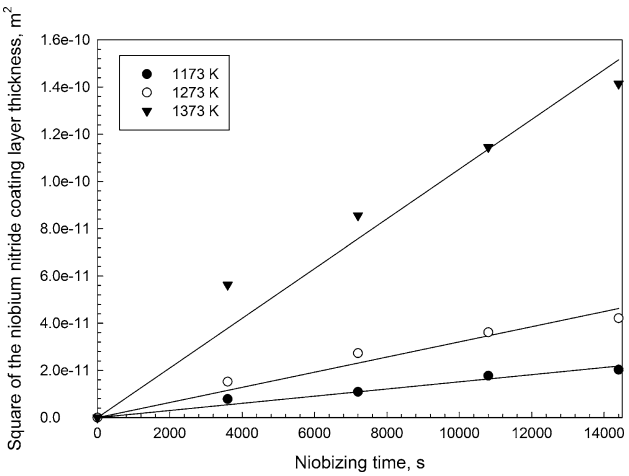

Fig. 7 Square of the niobium nitride layer thickness of nitro-niobized AISI 1010 steel vs. treatment time

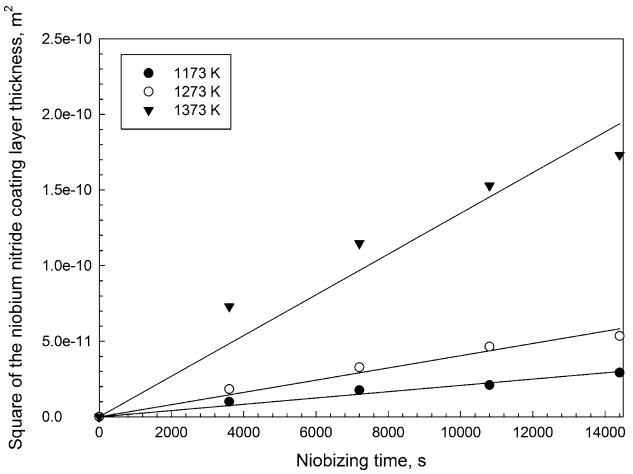

Fig. 8 Square of the niobium nitride layer thickness of nitro-niobized AISI D2 steel vs. treatment time

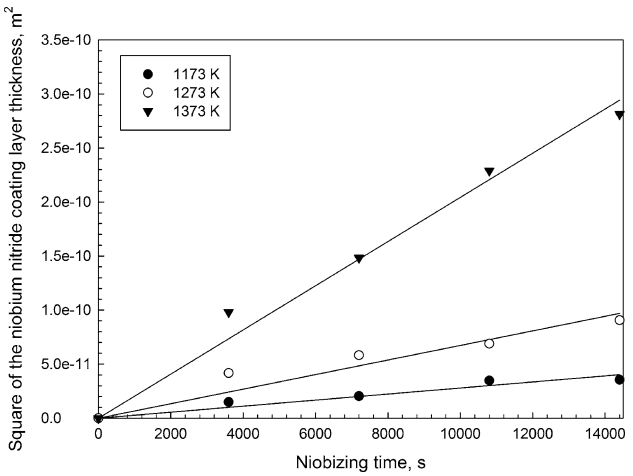

Fig. 9 Square of the niobium nitride layer thickness of nitro-niobized AISI M2 steel vs. treatment time

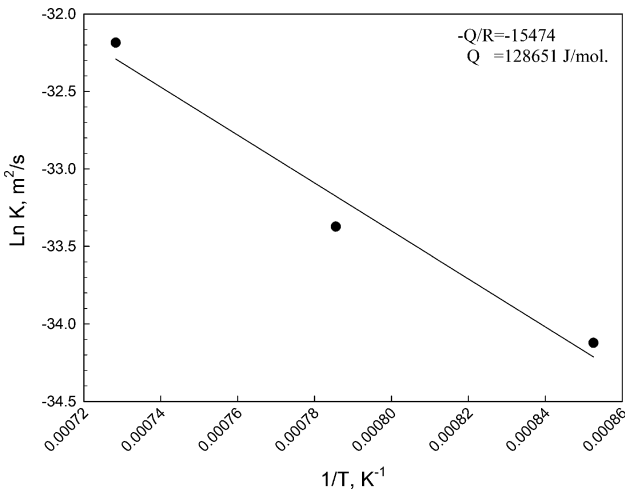

Fig. 10 Growth rate constant vs. temperature of nitro-niobized AISI 1010 steel

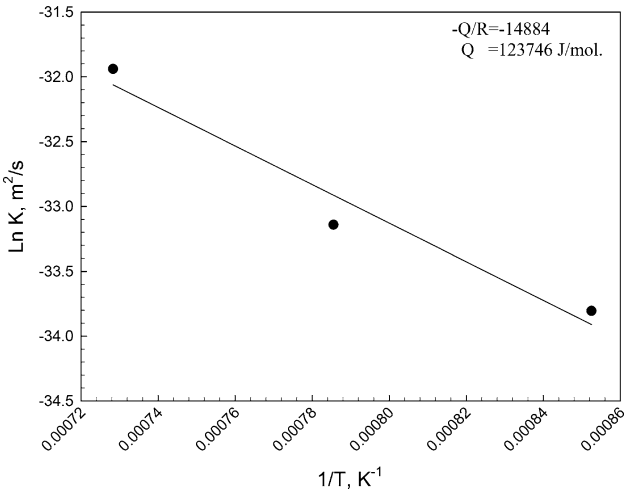

Fig. 11 Growth rate constant vs. temperature of nitro-niobized AISI D2 steel

slope of the plot ln$K$ vs $1/T$, using Eq. 3. The plot of ln$K$ vs. reciprocal niobizing temperature is thus shown to be linear in Figs. 10, 11, and 12; activation energy (Q) and K_o were determined from the slopes of straight lines obtained at $1/T = 0$ by setting the intercept of the extrapolated straight lines to the abscissa as the origin; the results are listed in Table 4. There are a lot of studies on the kinetics of the coatings realized by thermo-reactive diffusion technique. Some diffusion data, for coatings realized by thermo-reactive deposition technique are given in Table 5.

The growth rate of niobium nitride layer is controlled by niobium diffusion in the coating layer and niobium nitride layer growth occurs as a consequence of niobium diffusion perpendicular to the surface of the specimen. Fick's laws establish the concentrations of niobium in the niobium nitride layer. These laws take diffusion coefficient K into

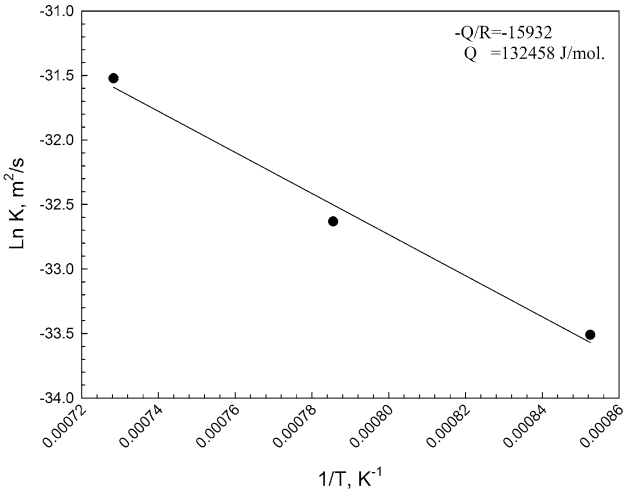

Fig. 12 Growth rate constant vs. temperature of nitro-niobized AISI M2 steel

Table 4 Growth rate constant (K) and activation energy (Q) as a function of steels and process temperature

Niobium nitride coated steels	Growth rate constant (m^2/s)			Activation energy (kJ/mol)
	1173 K	1273 K	1373 K	
AISI 1010	1.517×10^{-15}	3.209×10^{-15}	1.052×10^{-14}	128.7
AISI D2	2.082×10^{-15}	4.043×10^{-15}	1.346×10^{-14}	123.8
AISI M2	2.797×10^{-15}	6.735×10^{-15}	2.043×10^{-14}	132.5

Table 5 Kinetic data for some thermo-reactive diffusion coatings

Coating	Diffusion coefficient, K (m^2/s)	Activation energy, Q (kJ/mol)	
$NbC_{1073–1273\ K}$	2.11×10^{-15} to 1.03×10^{-14}	91.3	[28]
$TiN_{1173–1273\ K}$	6.64×10^{-15} to 2.10×10^{-14}	181.6	[34]
$VN_{1073\text{-}1273\ K}$	5.16×10^{-15} to 1.99×10^{-14}	75.9	[35]
$Cr_xC_{1223–1323\ K}$	6.33×10^{-15} 5.01×10^{-14}	278	[36]
$VC_{1223–1423\ K}$	3.40×10^{-15} to 2.80×10^{-14}	173.2	[37]
$VNC_{1223–1423\ K}$	1.15×10^{-14} to 1.02×10^{-13}	145.5	[23]
$Cr_xC_{1223–1423\ K}$	1.25×10^{-16} to 1.10×10^{-14}	281.6–399.6	[38]

account the as the parameter that determines the speed of formation of niobium nitride layers on steels. The K diffusion coefficient depends on the temperature of the process (according to the Arrhenius equation), the diffused niobium concentration on the surface, and the content of alloying elements in the steels [35, 36].

Conclusions

Niobium nitride coating of AISI 1010, AISI D2, and AISI M2 steels were performed using nitro-niobizing treatment. The following conclusions can be deduced from the present study:

1. Niobium nitride coating can be formed on the pre-nitrided steel samples by TRD method.
2. The niobium nitride layers formed on pre-nitrided steels show that coating layers formed on the steel samples include compact layers on the top and sub-layer, while the mid-layer of the coatings are a spongy structure. Coating layers are also well bonded to the substrate and crack free.
3. The longer the treatment time and the higher the treatment temperature, the thicker the niobium nitride layer became. Increases in alloying element in the steel substrate resulted to thicker coating layer.
4. The hardness of niobium nitride coating layers formed on the pre-nitrided steels are 1.38–10.12 times higher than that of the uncoated steels.
5. The growth rate constants and activation energies of the niobium nitride layers under the process conditions were very close to each other for all the steels compositions.
6. Contour diagrams derived from the coating layer thickness of the steels give good results depending on process parameters.

References

1. Ma J, Du Y, Qian Y (2005) J Alloys Compd 389:296
2. Elangovan T, Kuppusami P, Thirumurugesan R, Ganesan V, Mohandas E, Mangalaraj D (2010) Mater Sci Eng B 167:17
3. Hultman L (2000) Vacuum 57:1
4. Bendavid A, Martin PJ, Kinder TJ, Preston EW (2003) Surf Coat Technol 163–164:347
5. Rodil SE, Olaya JJ, Muhl S, Bhushan B, Wei G (2007) Surf Coat Technol 201:6117
6. Fenker M, Balzer M, Büchi RV, Jehn HA, Kappl H, Lee JJ (2003) Surf Coat Technol 163–164:169
7. Torche M, Schmerber G, Guemmaz M, Mosser A, Parlebas JC (2003) Thin Solid Films 436:208
8. Barshilia HC, Deepthi B, Rajam KS, Bhatti KP, Chaudhary S (2008) J Mater Res 23:1258
9. Benkahoul M, Martinez E, Karimi A, Sanjinés R, Lévy F (2004) Surf Coat Technol 180–181:178
10. Sandu CS, Benkahoul M, Parlinska WM, Sanjinés R, Lévy F (2006) Surf Coat Technol 200:6544
11. Klingenberg ML, Demaree JD (2001) Surf Coat Technol 146–147:243
12. Cappuccio G, Gambardella U, Morone A, Orlando S, Parisi GP (1997) Appl Surf Sci 109–110:399
13. Sproul WD (1996) Surf Coat Technol 81:1
14. Rutherford KL, Hatto PW, Davies C, Hutchings IM (1996) Surf Coat Technol 86–87:472
15. Sen S, Sen U, Bindal C (2005) Surf Coat Technol 191:274
16. Elers KE, Saanila V, Soininen PJ, Li WM, Kostamo JT, Haukka S, Juhanoja J, Besling WFA (2002) Chem Vapor Depos 8(4):149
17. Katsura M (1992) J Alloys Compd 182(1):91
18. Newport AC, Bleau JE, Carmalt CJ, Parkin IP, O'Neill SA (2004) J Mater Chem 14:3333

19. Harjanto lS, Shibayama A, Sato K, Suzuki G, Otomo T, Takasaki Y, Fujita T (2005) Resour Process 52:113
20. Sato N, Nanjo M (1985) Metallurg Trans B 16B:639
21. Dutta B, Sellars CM (1987) Mater Sci Technol 3:197
22. King PC, Reynoldson RW, Brownrigg A, Long JM (2004) J Mater Eng Perform 13(4):431
23. Aghaie-Khafri M, Fazlalipour F (2008) Surface Coat Technol 202:4107
24. Pei XJ, Zhen-Ming H, Shao-Bo F (1990) Materialwissenschaft und Werkstofftechnik 21(7):287
25. Brauner G (1962) Metal Sci Heat Treat 4(5–6):210
26. Wong MS, Sproul WD, Chu X, Barnet SA (1993) J Vac Sci Technol A 11(4):1528
27. Sen U, Sen S, Yilmaz F (2004) Surf Coat Technol 176:222
28. Ozbek I, Bindal C (2002) Surf Coat Technol 154:14
29. Tsipas DN, Rus J (1987) J Mater Sci Lett 6:118
30. Deniz G (2004) MSc Thesis, Sakarya University, Graduate School of Science, Sakarya
31. Fujita N, Bhadeshia HKDH (1999) Mater Sci Technol 15(6):627
32. Sen U (2004) Mater Chem Phys 86:189
33. Chen FS, Wang KL (1999) Surf Coat Technol 115:239
34. Bouayad A, Gerometta CH, Belkebir A, Ambari A (2003) Mater Sci Eng A 363:53
35. Meléndez E, Campos I, Rocha E, Barrón MA (1997) Mater Sci Eng A 234–236:900
36. Brakman CM, Gommers AWJ, Mittemeijer EJ (1989) J Mater Res 4–6:1354
37. Genel K, Ozbek I, Kurt A, Bindal C (2002) Surf Coat Technol 160:38
38. Wei CY, Chen FS (2005) Mater Chem Phys 91:192